Saudi Pharmaceutical Journal 27 (2019) 25–32

Contents lists available at ScienceDirect

Saudi Pharmaceutical Journal

journal homepage: www.sciencedirect.com

Original article

Predicting the content of anthraquinone bioactive in Rhei rhizome (*Rheum officinale* Baill.) with the concentration addition model

Zeyad Alehaideb [a,*], Kimberly C. Chin [b], Mei Cun Yao [c], Francis C.P. Law [b]

[a] Department of Medical Genomics, King Abdullah International Medical Research Center/King Saud Bin Abdulaziz University for Health Sciences, PO Box 22490, Riyadh 11426, Saudi Arabia
[b] Department of Biological Sciences, Simon Fraser University, Burnaby, B.C. V5A 1S6, Canada
[c] School of Pharmaceutical Sciences, Sun Yat-Sen University, Guangzhou, Guangdong 510006, China

ARTICLE INFO

Article history:
Received 29 January 2018
Accepted 19 July 2018
Available online 20 July 2018

Keywords:
Rhei rhizome
Anthraquinone
Cytochrome P-450 inhibition

ABSTRACT

Rhei rhizome (*Rheum officinale* Baill.) (RR) contains a large number of anthraquinone bioactive, yet little is known of the combined effect of these anthraquinones in a mixture. The goals of this study were: to determine the inhibitory potencies of individual anthraquinones and whole RR extract against human liver microsomal CYP1A2/3A4 activity, to predict the content of anthraquinones in RR using the concentration addition (CA) model, and to compare predicted and empirical contents in the same RR sample. Anthraquinone concentrations in the RR extract were determined using HPLC. The inhibitory potencies of individual anthraquinones were determined in incubations containing human liver microsomes. The study results were used to predict an effect-based dose measure of the anthraquinones in RR using the CA model. An empirical dose measure also was determined in the whole RR extract using the CYP1A2/3A4-based bioassay. For the CYP1A2-based studies, the predicted and empirical dose measures of anthraquinones were identical; they were 12.0 ± 1.80 and 12.20 ± 0.81 mg aloe-emodin equivalents/g RR, respectively. For the CYP3A4-based studies, the predicted and empirical dose measures were different; they were 2.80 ± 0.10 and 19.04 ± 0.41 mg aloe-emodin equivalents/g RR, respectively. Only the CYP1A2-based CA model which assumed additive effects of RR anthraquinones predicted an effect-based dose measure that was verifiable by empirical data. The CA model provides an alternative approach to the CYP1A2/3A4-based bioassay or empirical method to screen for the anthraquinones in RR. The CA model as described in this study is applicable to other botanical drugs, plant-based foods and dietary supplements.

1. Introduction

Rhei rhizome (RR), the roots and rhizomes of *Rheum officinale* Baill (Pharmacopoeia of China, 2000), is an herbal medicine for the treatment of catharsis, fever, infection, inflammation, and cancer in China, Japan and Korea (Huang, 1999). The extract and decoction of RR contains many anthraquinone bioactive chemicals (ABCs) including aloe-emodin (AEM), emodin, rhein, chrysophanol, and physcion (Fig. 1) (Huang, 1999; Yan et al., 2008) and the pharmacological and toxicological effects of RR are believed resulting from the combined effects of the ABCs.

The pharmacokinetics of individual ABCs and RR extracts has been studied in different animal species (Dahms et al., 1997; Yan et al., 2008). Almost all these pharmacokinetic studies are carried out with one of the ABCs; only a few studies are conducted using the whole RR extract. The ABCs of RR are absorbed rapidly into the blood of rats after oral administration; peak anthraquinone concentrations usually appear in the plasma within 0.5 hr post-dosing (Yan et al., 2008). The ABCs are metabolized by laboratory animals and humans primarily to glucuronide and sulfate conjugates (Shia et al., 2009; Dahms et al., 1997) although a small amount of the ABCs is metabolized by CYP1A2 isozyme in the liver (Dahms et al., 1997; Mueller et al., 1998). CYP3A4-mediated metabolism of RR ABCs has never been reported in humans prior to the present study.

Dose is a fundamental concept in pharmacology; yet scientists are still grappling with the definition and the measurement of dose for a botanical drug. The USFDA defines the dose of an herbal product as the total weight of plant materials administered to humans (USFDA, 2004), which contains not only the bioactive

* Corresponding author.
E-mail address: alehaidebze1@ngha.med.sa (Z. Alehaideb).
Peer review under responsibility of King Saud University.

Production and hosting by Elsevier

https://doi.org/10.1016/j.jsps.2018.07.015
1319-0164/

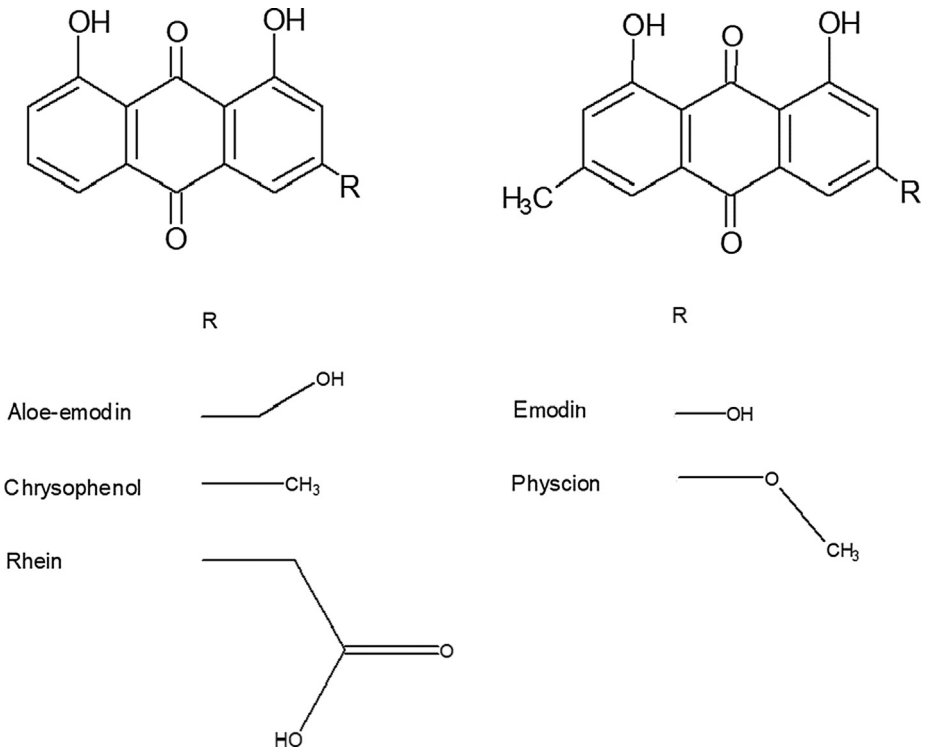

Fig. 1. Chemical structures of major anthraquinone bioactive in *Rhei rhizome*.

chemicals but also the inactive chemicals, plant cells, and fibers. As such, the total dose of a botanical drug remains unknown although most bioactive chemicals can be quantified by chemical analysis which provides little or no information on the combined effects of a chemical mixture. Recently, the CYP450-based bioassay has been used to study the relationship between a mixture of bioactive chemicals in an herbal extract and the inhibition of hepatic microsomal CYP450 isozymes by treating the chemical mixture as a single chemical entity (Foster et al., 2002). More recently, Strandell et al., 2004, define the inhibitory potency (IC_{50}) of an herbal product as the dilution volume of the herbal extract which contains extractable activity from a recommended human dose invoking a half-maximal inhibition toward a specific hepatic CYP450 isozyme (liters/dose unit).

The goals of this study were to: study the IC_{50} of pure RR anthraquinones and whole RR extract toward human liver microsomal CYP1A2/3A4 activity *in vitro*, predict an effect-based dose measure for the ABCs in RR with the concentration addition (CA) model (ATSDR, 2004; USEPA, 1999), and compare model-predicted dose with empirical dose in the same RR sample. The CA model is able to relate measured chemical concentrations to the additive effects of a chemical mixture (ATSDR, 2004; USEPA, 1999). It has been widely used to predict the effect-based dose measure for chemical mixtures in the environment. Results of our study show care must be exercised in choosing an appropriate CYP450 isozyme to implement the CA model since only the CYP1A2 isozyme, not the CYP3A4 isozyme, is able to predict an effect-based dose measure for the ABCs that is verifiable by empirical data.

2. Materials and methods

2.1. Chemicals, RR and human liver microsomes

RR was purchased from a local Chinese herbal medicine store in Guangzhou, China. It was authenticated by Dr. Mei Cun Yao, School of Pharmaceutical Sciences, Sun Yat-Sen University (Guangzhou, China). A voucher sample was kept in his laboratory. RR was extracted by ethanol and dimethyl sulphoxide (DMSO); they were analyzed by HPLC and found to be free of common pesticides and environmental pollutants.

AEM, emodin, rhein, caffeine, erythromycin, and β-nicotinamide adenine dinucleotide phosphate (β-NADPH) were obtained from Sigma-Aldrich Canada Ltd. (Mississauga, ON). Chrysophanol and physcion were purchased from ChromaDex (Los Angeles, CA). Purities of the anthraquinone standards were >95%. Standard solutions were prepared by dissolving a known amount of pure anthraquinone in DMSO. Pooled human liver microsomes were purchased from Becton Dickinson (NYC, NY). Supelclean Envi-Carb® solid phase extraction (SPE) columns were purchased from Supelco Canada Ltd. (Oakville, ON). Dipotassium phosphate (K_2HPO_4), disodium phosphate (Na_2HPO_4), and trichloroacetic acid (TCA) were purchased from Anachemia (Norman Lachine, QC). Ethanol was purchased from Commercials Alcohol (Toronto, ON). DMSO, mono-potassium phosphate (KH_2PO_4), methanol and acetonitrile were obtained from Caledon (Bolton, ON). Research grade water was produced using a Millipore system (Billerica, MA, USA) with a minimum resistivity of 16.0 MΩ cm at 25 °C.

[1-^{14}C-Methyl]-caffeine (specific activity 55 mCi/mmol, radiochemical purity > 99%), [*N*-methyl-^{14}C]-erythromycin (specific activity 48.8 mCi/mmol, radiochemical purity >97%) and liquid scintillation cocktail were purchased from Perkin Elmer Life Sciences and Analytical Services, Inc. (Wellesley, MA). Prior to use, [1-^{14}C-methyl]-caffeine was purified using a 3-ml Supelclean Envi-Carb® solid-phase extraction column as described by Bloomer et al. (1995).

2.2. RR extracts

Two grams of minced RR were extracted by 40 ml of ethanol in a Branson sonicator (Shelton, CT) for 2 hr at room temperature. The mixture was filtered using a 0.45-μm Millipore Centrifree® Ultrafiltration device. About 30 ml of the filtered solution was analyzed by

the HPLC. The remaining 10 ml filtered solution was dried, reconstituted in 2 ml of DMSO and used to determine the IC_{50} of the whole RR extract.

2.3. Determine anthraquinone concentrations in RR extract using HPLC

The filtered extract (see Section 2.2) was analyzed by a HPLC system consisting of Agilent ZORBAX Eclipse Plus-C18 95 Å reverse-phase column (4.6 × 250 mm *i.d.*, 5 μm), vacuum degasser, binary pump, autosampler, fluorescence detector (FLD) and HP1090 series Chemstation (Palo Alto, CA). The excitation and emission wavelengths of the FLD were set at 435 nm and 515 nm, respectively. The anthraquinone bioactive were eluted from the HPLC column at room temperature using a solution of methanol-acetonitrile-0.2 M Na_2HPO_4 (27:35.5:37.5 v/v) at 1 ml/min flow rate. The external standard method was used to quantify the concentrations of ABCs in the extract. HPLC peak areas were linearly related to the amounts of pure anthraquinone injected; the coefficients of linearity of the ABCs were all >0.99. The highest concentrations used in the calibration curves were 0.24, 0.20, 0.43, 0.18, and 0.21 mg/ml for rhein, AEM, emodin, chrysophanol, and physcion, respectively. The limits of detection (LOD) for rhein, AEM, emodin, chrysophanol and physcion in the HPLC were 0.003, 0.002, 0.005, 0.009, and 0.004 mg/ml, respectively. The LOD were determined using the B.E.N. Software (Version 2.0, Institute of Legal Medicine and Traffic Medicine, Germany. DIN 32645).

2.4. In vitro inhibition of human liver microsomal CYP1A2/CYP3A4 activity by pure anthraquinones and whole RR extract

The IC_{50} of pure anthraquinones and whole RR extract were determined under similar incubation conditions except the IC_{50} of pure anthraquinones were based on anthraquinone concentration and the IC_{50} of whole RR extracts were based on extract dilution volume. ^{14}C-caffeine (Bloomer et al., 1995) and ^{14}C-erythromycin (Riley and Howbrook, 1998) were used as the probe substrates for measuring CYP1A2 and CYP3A4 enzymic activity, respectively.

A typical incubation mixture consisted of [1-^{14}C-methyl]-caffeine (0.75 μCi, 250 μM) or [*N*-methyl-^{14}C]-erythromycin (0.5 μCi, 60 μM), 0.25 mg human liver microsomes, 0.002 ml of the test solution (anthraquinone standard solution or RR extract), and NADPH in 50 mM phosphate buffer (pH 7.4) to give a final incubation volume of 0.2 ml. Incubation was performed in a 37 °C Dubnoff water bath with shaking at 60 cycles/min. After a 5 min pre-incubation period, the reaction was initiated by the addition of human liver microsomes. The reaction was allowed to continue for an additional 20 min (CYP3A4) or 25 min (CYP1A2) before being stopped by adding 50 μl of 10% TCA.

The incubation mixture was centrifuged at 3500 rpm for 5 min to separate protein precipitates from the supernatant. A 150 μl aliquot of the supernatant was applied to a pre-conditioned SPE column. [^{14}C]-Formaldehyde and/or [^{14}C]-formic acid, the metabolites from ^{14}C-caffeine and ^{14}C-erythromycin demethylation, were eluted from the SPE column with 2 ml of water into a liquid scintillation vial. After adding 15 ml of liquid scintillation fluid, the radioactivity in the vial was quantified using a liquid scintillation counter. CYP1A2/3A4 activity inhibition was expressed as the residual activity of control incubation *i.e.*, incubation without anthraquinone.

2.5. Determining IC_{50} and relative potency

The IC_{50} was determined from the CYP1A2/3A4 activity inhibition *vs.* anthraquinone concentration (or RR extract dilution volume) plots. CYP1A2/3A4 inhibition data were first normalized from 0% to 100% and then plotted against log anthraquinone concentration (or log extract dilution volume). The resulting dose-response curves were fitted separately to a four-parameter logistic function (Eq. (1) to determine the IC_{50} values. Curve fitting was performed using the GraphPad Prism (Version 5.0, GraphPad Software, San Diego, CA. USA). The IC_{50} represented the concentration of a pure anthraquinone (or the dilution volume of RR extract), which evoked a half-maximal inhibition of CYP1A2/3A4 activity.

$$\text{Response} = \text{Min} + (\text{Max} - \text{Min})/[1 + 10^{(\log IC_{50} - \log c)(-m)}] \quad (1)$$

Where response represents 50% maximum inhibition; log c, the logarithm of a pure anthraquinone concentration (or dilution volume of RR extract); max and min, respectively, are the 100% and 0% inhibition of the concentration (or dilution volume)-inhibition curve; m, the Hill slope.

The relative potency (RP) of an anthraquinone (or RR extract) represented an equally effective AEM concentration for CYP1A2/3A4 activity inhibition. The RP of an anthraquinone was calculated based on the ratio of (AEM IC_{50})/(another anthraquinone IC_{50}). Parallelism between the inhibition-log concentration curves of both anthraquinones was a basic requirement for determining an accurate RP value for the pure anthraquinone (Villeneuve et al., 2000).

Similarly, the RP of the whole RR extract was calculated based on the ratio of (AEM IC_{50})/(extract IC_{50}). Also, parallelism between the inhibition-log sample dilution volume curve and the inhibition-log AEM concentration curve was required to determine an accurate RP value for the whole extract (Villeneuve et al., 2000).

2.6. Model-predicted integrated dose measure of ABCs in RR extract

The following equation describes the CA model for a mixture of *n* chemical components (ATSDR, 2004):

$$EC_{mix} = \left[\sum_{i=1}^{n} \frac{PXi}{ECi}\right] \quad (2)$$

where EC_{mix} is the total mixture concentration that is required to produce an effect. *PXi* is the concentration of the *ith* compound relative to total mixture concentration, *ECi* is the equivalent effect concentration of a single substance that alone would produce the same effect as the mixture.

The CA model (Eq. (2) can be used to predict the total concentration of a chemical mixture based on the proportions of chemical concentrations and the IC_{50} of individual chemical constituents in the mixture. In applying the CA model with the toxic equivalency factor approach (Safe,1998), the response to the chemical mixture is assumed to be concentration additive, if it is equal to that produced by the dose of the first chemical alone. As such, the mixture dose/concentration can be expressed as the equivalent dose of the first chemical (ATSDR, 2004):

$$X = \sum_{i=1}^{n} Xi \text{ x } RPi \quad (3)$$

where *Xi* is the concentration of the i^{th} component. *RPi* is the IC_{50} of the i^{th} component relative to the first chemical.

The chemical structures of rhein, AEM, emodin, chrysophanol, and physcion are very similar (Fig. 1). Thus these ABCs have similar biological effects and mode of action. As a result, the total dose of ABCs in RR extract can be predicted by adding the concentrations of individual anthraquinones together after adjusting for the differences in RP values and the volume of extraction (VEE/DW):

$$(\text{AEM equivalents, mg/g})_{\text{predicted}} = \left(\sum_{i=1}^{n} Xi \text{ x } RPi\right)(\text{VEE/DW}) \quad (4)$$

where *Xi* represents the concentrations/doses of individual in RR extract, which are determined by HPLC (mg/ml); *RPi* represents the relative potency calculated from the ratio of AEM IC_{50}/another anthraquinone IC_{50}; VEE is the volume of ethanol used to extract RR (ml); DW is dried weight of RR used in ethanol extraction (g).

2.7. Empirical integrated dose measure of ABCs in RR extract

The content of ABCs in RR also could be determined experimentally from the RP of the whole extract. In the present study, the AEM concentration-inhibition curve and the whole extract dilution volume-inhibition curve were determined simultaneously to minimize potential experimental errors. The following equation was used to calculate the empirical dose measure of anthraquinones in RR (Lorenzen et al., 2004):

$$(\text{AEM equivalents, mg/g})_{\text{empirical}} = (\text{AEM } IC_{50}/\text{whole extract } IC_{50})\text{x}(\text{VAM}/\text{VET})\text{x}(\text{VRD}/\text{DWR}) \quad (5)$$

where AEM IC_{50}, the IC_{50} of an AEM standard solution (mg/ml); whole extract IC_{50}, the IC_{50} of RR extract in dilution volume (unitless); VAM, the volume of liver microsomal incubation mixture (ml); VET, the volume of extract tested (ml); VRD, the volume of DMSO to re-dissolve extracted residues (ml); DWR, RR dried weight in the volume of DMSO (g). Eq. (5) determined the equivalent amount of AEM that would elicit the same inhibitory effect as the mixture of ABCs in RR.

2.8. Statistical analysis

Results of anthraquinone concentrations in RR extract and CYP1A2/3A4 inhibition studies were reported as mean ± SD of three independent experiments.

3. Results

3.1. Quantifying individual anthraquinone bioactive in RR extract using HPLC

Fig. 2A shows a typical HPLC chromatogram for a mixture of anthraquinone standards in DMSO. The retention times of rhein, AEM, emodin, chrysophanol, and physcion were 8.13, 8.39, 20.66, 31.52, and 48.31 min, respectively. Fig. 2B depicts a typical HPLC chromatogram of the RR extract. The HPLC peaks were identified initially by retention times; they were later confirmed by spiking with anthraquinone standards. Table 1 summarizes the concentrations of major anthraquinones in the RR extract. A chemical dose of 17.8 mg/g RR was calculated by adding up the concentrations of individual anthraquinones in the extract and dividing the sum with

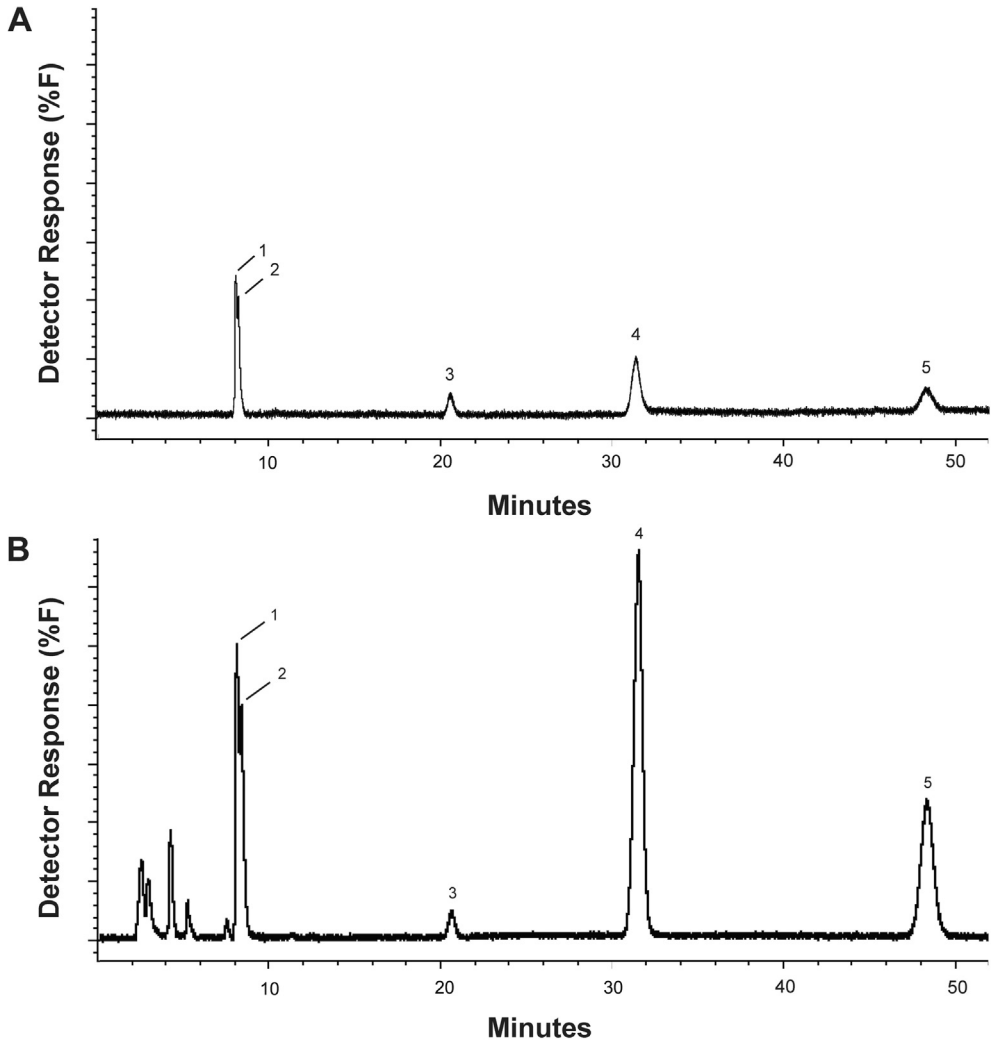

Fig. 2. HPLC chromatograms of a mixture of pure anthraquinones and *Rhei rhizome* extract. (A) a mixture of pure anthraquinones, and (B) *Rhei rhizome* extract. (1) Rhein, (2). AEM, (3) Emodin, (4) Chrysophanol, (5). Physcion.

Table 1
Concentrations of anthraquinone bioactive in RR extract*

Anthraquinone bioactive	Concentration in *Rhei rhizome* extract (mg/ml)**
Rhein	0.218 ± 0.004
Emodin	0.101 ± 0.006
Aloe-emodin	0.067 ± 0.003
Chrysophanol	0.266 ± 0.018
Physcion	0.238 ± 0.006

* Two grams of *Rhei rhizome* were extracted by 40 ml of ethanol.
** Data represent mean ± SD of three independent experiments.

the dried weight of RR (2 g) used in extraction. The chemical dose was higher than the CA model-predicted dose measures (see Section 3.5) because it did not account for the inhibitory effects of the anthraquinones.

3.2. Concentration-inhibition curves of pure anthraquinones

Fig. 3 depicts the inhibition-log concentration profiles of individual anthraquinones toward CYP1A2-mediated caffeine-*N*-demethylase activity. These profiles showed a sigmoidal relationship between CYP1A2 activity inhibition and added anthraquinone. The inhibition-log concentration curves of the ABCs, with the exception of physcion, were parallel to one another with equal maxima (100%) and minima (0%).

Fig. 4 shows the inhibition-log concentration profiles of individual anthraquinones toward CYP3A4-mediated erythromycin-*N*-demethylase activity. These profiles also showed a sigmoidal relationship between added anthraquinone and CYP3A4 activity inhibition. However, no inhibition-log concentration curves could be constructed for chrysophanol and physcion since they had little or no inhibitory effects on CYP3A4 activity. Also, only the inhibition-log concentration curves of emodin and AEM were parallel to each other.

3.3. IC_{50} and RP of pure anthraquinones

Table 2 summarizes the IC_{50} and RP values of individual ABCs in RR. The small IC_{50} of rhein, AEM, physcion and chrysophanol indicated they were potent inhibitors of CYP1A2 activity. The large IC_{50} of emodin indicated that it was a weak CYP1A2 inhibitor. In contrast, emodin and AEM were moderate inhibitors of CYP3A4

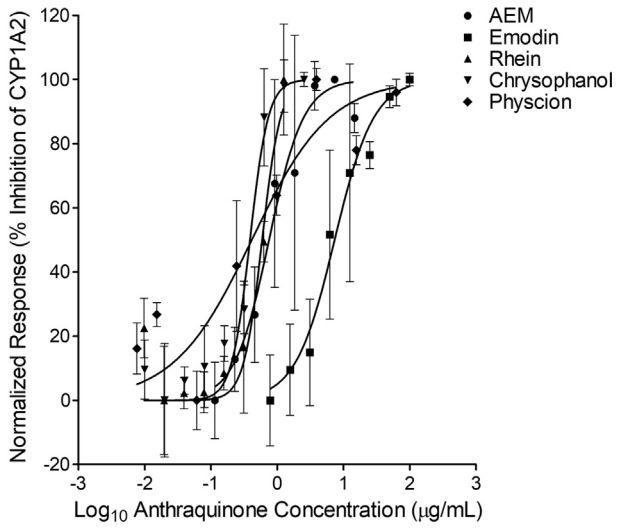

Fig. 3. Inhibition of CYP1A2-mediated caffeine-*N*-demethylase activity by anthraquinone standards. Results are expressed as mean ± SD of three independent studies. Experimental details are described under "Materials and methods".

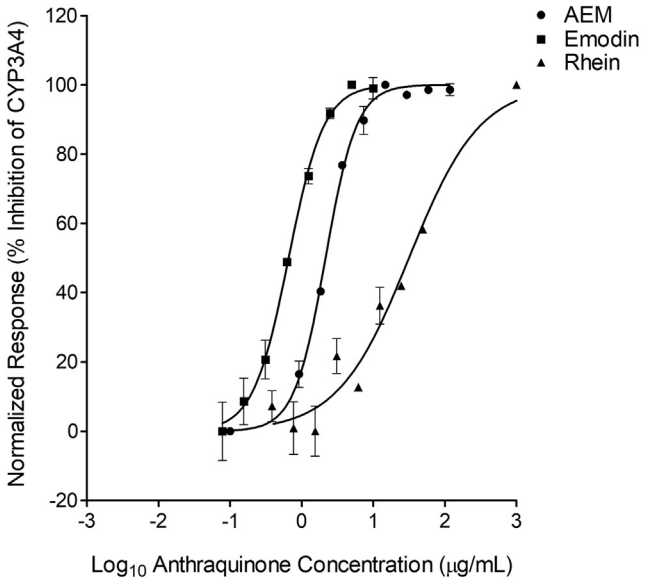

Fig. 4. Inhibition of CYP3A4-mediated erythromycin-*N*-demethylase activity by anthraquinone standards. Results are expressed as mean ± SD of three independent studies. Experimental details are described under "Materials and methods".

Table 2
IC_{50} and RP values of pure anthraquinones based on *in vitro* inhibition of caffeine demethylase and erythromycin demethylase activities.

Anthraquinone bioactive	*In vitro* IC_{50}, μg/ml and [relative potency, unitless]*	
	CYP1A2-mediated Caffeine demethylation	CYP3A4-mediated Erythromycin demethylation
Rhein	0.62 ± 0.01 [0.68]	27.75 ± 1.35 [0.08]
Emodin	18.10 ± 5.00 [0.02]	4.10 ± 0.37 [0.55]
Aloe-emodin	0.42 ± 0.06 [1.00]	2.24 ± 0.06 [1.00]
Chrysophanol	0.44 ± 0.01 [0.96]	>69.0** [<0.03]
Physcion	0.43 ± 0.00 [0.98]	>62.5** [<0.04]

* IC_{50} values represent the mean ± SD of three independent experiments except when otherwise indicated. Bracketed values represent RP of individual anthraquinones using AEM as the reference chemical *i.e.*, (AEM IC_{50})/(other anthraquinone IC_{50}).
** Results from two independent experiments.

activity and rhein, chrysophanol and physcion were weak inhibitors of CYP3A4 activity. Because AEM was a potent and moderate inhibitor of CYP1A2 activity and CYP3A4 activity, respectively (Table 2), it was chosen the reference chemical to calculate the RP for other anthraquinones.

The RP values of individual anthraquinones confirmed the IC_{50} results (Table 2). The relatively high RP values of rhein, chrysophanol and physician showed that they were potent inhibitors of CYP1A2 activity and the small RP of emodin confirmed it was a weak inhibitor of CYP1A2 activity. The small RP values of rhein, chrysophanol, and physcion suggested they had little or no inhibitory effects on CYP3A4 activity (Table 2). However, the high RP value of emodin showed it was a moderate inhibitor of CYP3A4 activity.

We also examined the inhibitory effects of dimeric sennosides A and B toward CYP1A2/3A4 activity. Sennoside A was a weak inhibitor of CYP3A4 and CYP1A2 activities; it had IC_{50} values >179.3 μg/ml and >134.0 μg/ml, respectively. Sennoside B was a moderate inhibitor of CYP3A4 and CYP1A2 activities; it had IC_{50} values 15.38 and 28.59 μg/ml, respectively.

3.4. IC_{50} and RP of whole RR extract

Fig. 5 shows the CYP1A2 inhibition-log AEM concentration curve and the CYP1A2 inhibition-log RR extract dilution volume curve are parallel to each other; the slopes of the curves are 1.74 and 1.77, respectively. The IC_{50} of whole RR extract was 0.014 ± 0.001 sample dilution volume which equated to a RP value of 30.0 μg AEM equivalents/ml.

Fig. 6 shows the CYP3A4 inhibition-log AEM concentration curve and the CYP3A4 inhibition-log RR extract dilution volume curve are not parallel to each other; the slopes of the curves are 1.89 and 2.30, respectively. The IC_{50} of the whole RR extract was

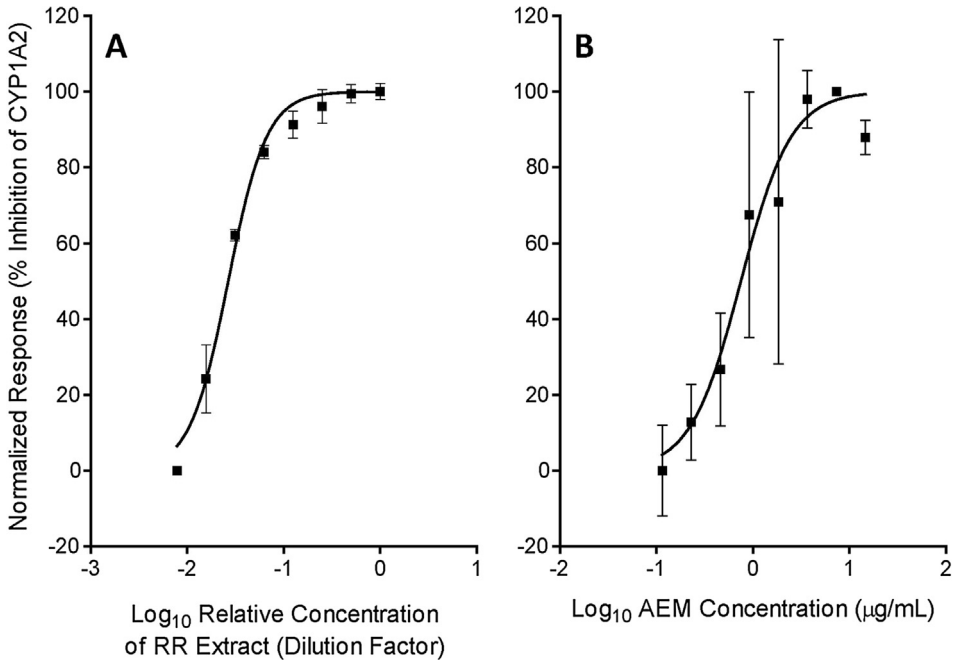

Fig. 5. Inhibition of CYP1A2-mediated caffeine-*N*-demethylase activity by (A) *Rhei rhizome* extract, (B) AEM. Results are expressed as mean ± SD of three independent studies. Experimental details are described under "Materials and methods".

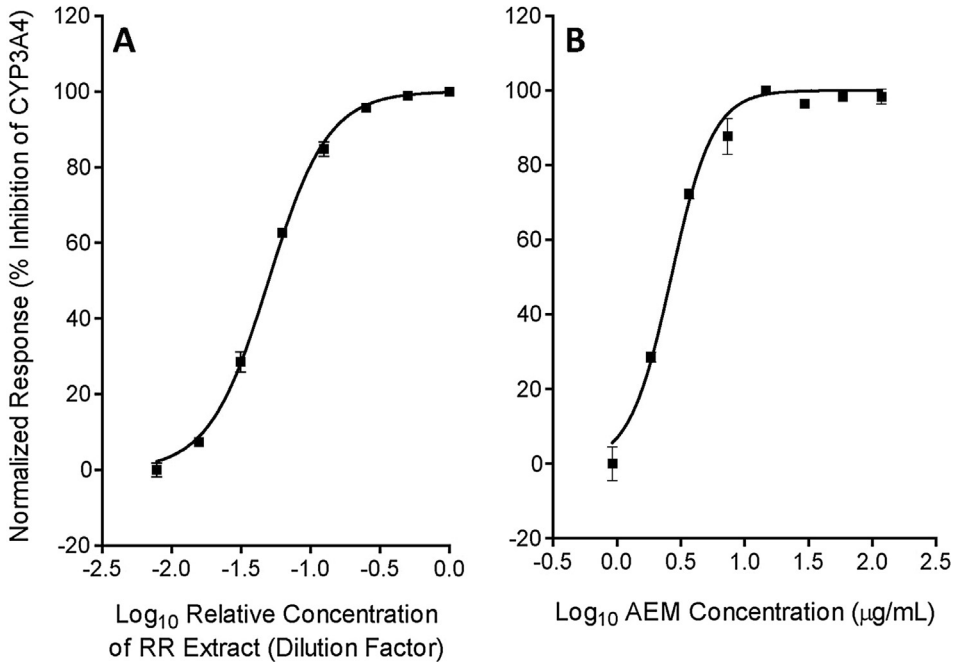

Fig. 6. Inhibition of CYP3A4-mediated erythromycin-*N*-demethylase activity by (A) *Rhei rhizoma* extract, (B) AEM. Results are expressed as mean ± SD of three independent studies. Experimental details are described under "Materials and methods".

0.047 ± 0.001 sample dilution volume which equated to a RP of 47.7 μg AEM equivalents/ml.

3.5. Model-predicted and empirical contents of ABCs in RR extract

The effect-based dose measure of the anthraquinone mixture in RR was predicted using the CA model or determined experimentally using the CYP450-based bioassay. The predicted and experimental dose measures were very close to identical if the IC_{50} were determined using the CYP1A2 isozyme; they were 12.0 ± 1.80 and 12.20 ± 0.81 mg AEM equivalents/g RR, respectively. In contrast, the predicted and experimental dose measures were different if the IC_{50} were determined using the CYP3A4 isozyme; they were 2.80 ± 0.10 and 19.04 ± 0.41 mg AEM equivalents/g RR, respectively.

4. Discussion

We have identified and quantified five major anthraquinones in the ethanolic extract of RR (Table 1). The same five anthraquinones have been reported in other RR extracts and decoctions (Koyama et al., 2005). The IC_{50}/RP of pure anthraquinones are determined using ^{14}C-labeled probe substrates (Table 2) since radiometric analysis significantly reduces false positive results due to intrinsic fluorescence of the anthraquinones (Yan et al., 2008; Zou et al., 2002). In the present study, CYP1A2 and CYP3A4 isozymes are used to examine the inhibitory effects of RR extract and its bioactive components because ABCs are metabolized by CYP1A2 (Dahms et al., 1997; Mueller et al., 1998) and CYP3A4 constitutes about 47% of the CYP450 in the liver of humans (Venkatakrishnan et al., 2001). Therefore, although CYP3A4-mediated ABCs metabolism has not been reported in previous studies, it is included in the present study.

The predicted and empirical dose measures for ABCs in the RR extract are identical if CYP1A2 were used to determine the IC_{50} values. In contrast, the predicted and empirical dose measures are different if CYP3A4 were used to determine the IC_{50} values (Section 3.5). An explanation for the different dose measures in the CYP1A2-based and CYP3A4-based studies is not available but probably is related to the structural and functional differences of these isozymes and the parallelism between the inhibition-concentration curves (Figs. 3–6):

4.1. Structural and functional difference of CYP1A2 and CYP3A4

Firstly, ABCs in RR are moderate or potent inhibitors of human liver microsomal CYP1A2 activity (Table 2). These results are consistent with the findings that phase I anthraquinones metabolism mainly involves hepatic CYP1A2 isozyme (Dahms et al., 1997; Mueller et al., 1998) and 2, 6-dihydroxyanthraquinone is a potent inhibitor of rat liver microsomal CYP1A1/2 activity *in vitro* (Ayrton et al., 1987). Lewis and Lake (1996) have shown that co-planar substrates *e.g.*, caffeine and anthraquinones are bound specifically to the rectangular active sites of CYP1A2, which lead to competitive inhibition of CYP1A2 activity.

Secondly, the anthraquinones are weak inhibitors of human liver microsomal CYP3A4 activity (Table 2). These results are consistent with the observation that no CYP3A4-mediated anthraquinone metabolism has been reported prior to our study (Dahms et al., 1997; Mueller et al., 1998). Guengerich (1999) reports that CYP3A4 is an isozyme which has broad substrate catalytic activity. The lack of substrate specificity may explain why the anthraquinones are weak inhibitors of CYP3A4 activity (Table 2). Perhaps, using a different CYP3A4-substrates such as testosterone or midazolam may yield a stronger inhibitory effect of the anthraquinones since different probe substrates are known to give different measurement outcomes (Foti et al., 2010).

All together these studies indicate that CYP1A2 is more relevant and appropriate than CYP3A4 in applying the CA model to predict an effect-based dose measure for the anthraquinones of RR. This conclusion is also supported by the degree of parallelism in the inhibition-concentration curves (see below).

4.2. Parallelism between inhibition-concentration (extract dilution volume) curves

Model-predicted dose measure depends on the RP value which in turn is dependent on whether the inhibition-log concentration curves of the test and reference chemicals are parallel to each other (Villeneuve et al., 2000). In the present study, the CYP1A2 inhibition-log concentration curves of individual anthraquinones, except physcion, are parallel to one another (Fig. 3). Thus, the RP values of the anthraquinones are accurately determined. As a result, the CYP1A2-based CA model is able to predict an effect-based dose measure that is verifiable by empirical data (Section 3.5). In contrast, only the AEM and emodin inhibition-log concentration curves are parallel in CYP3A4-based studies and no inhibition-log concentration curves can be constructed for chrysophanol and physcion (Fig. 4). Since both chrysophanol and physcion are excluded from the predicted dose measurement, the CYP3A4-based CA model predicts a much smaller dose measure than the empirical study (Section 3.5).

Similarly, the accuracy of empirical dose measures is dependent on parallelism between the inhibition-concentration and inhibition-extraction volume curves. For the CYP1A2 study, the inhibition-log AEM concentration and the inhibition-log extract dilution volume curves are parallel to each other with slopes of 1.74 and 1.77, respectively (Fig. 5). Thus, the CYP1A2-based bioassay is able to determine an effect-based dose measure identical to that of the CA model. For the CYP3A4 study, the inhibition-log AEM concentration and inhibition-log extract dilution volume curves are not parallel to each other; the slopes are 2.30 and 1.89, respectively (Fig. 6). As a result, the CYP3A4-based assay yields a large effect-based dose measure (Section 3.5) perhaps due to binding with unknown CYP3A4 substrates in the extract.

The CYP1A2-based CA model shows the content of anthraquinones in RR can be accounted for by adding just five anthraquinones (*i.e.*, rhein, AEM, emodin, chrysophanol and physcion) together (see Section 3.5). Other RR bioactive chemicals such as stilbene derivatives, tannic acids (Kashiwada et al., 1986), sennosides, *etc.*, do not seem to contribute significantly to the model-predicted dose measure (Sections 3.3 and 3.5) even though tannic acids have been shown to precipitate CYP450 isozymes (Yao et al., 2008).

This is the first study in which the CA model is used to predict an effect-based dose measure for a mixture of ABCs in RR. The CA model has many applications in research and development of herbal medicine; it can be used as an alternative to CYP1A2/3A4-based bioassay in determining the contents of ABCs in RR. It can also be used to predict the internal tissue dose measures (Andersen, 1987) of the ABCs in humans as described in our recent tea catechin mixture study (Law et al., 2017). The CA model is also applicable to the bioactive chemicals in plant-based foods, dietary supplements, and nutraceuticals.

Conflict of interest statement

The authors declare that there are no conflicts of interest.

Acknowledgements

This work was partially supported by the Natural Science Foundation of China grant (No. 30873428), the National Major Projects for Science and Technology Development from Science and Technology Ministry of China (No. 2009ZX09304-003), and the Saudi Arabian National Guard Health Affairs. F. C. P. Law thanked South China Normal University, Guangzhou, China for awarding a Study Leave research grant.

References

Andersen, M.E., 1987. Tissue dosimetry in risk assessment, or what's the problem here anyway? In: Pharmacokinetics in Risk Assessment, Drinking Water and Health. National Academy Press, Washington, D.C, pp. 8–23.

ATSDR. 2004. Guidance manual for the assessment of joint toxic action of chemical mixtures, Agency for Toxic Substances and Disease Registry, Public Health Service, U.S. Department of Health and Human Services.

Ayrton, A.D., Lewis, D.F., Ioannides, C., Walker, R., 1987. Anthraflavic is a potent and specific inhibitor of cytochrome P448 activity. Biochim. Biophys. Acta. 916, 328–331.

Bloomer, J.C., Clarke, S.E., Chenery, R.J., 1995. Determination of P4501A2 activity in human liver microsomes using [3-^{14}C-methyl] caffeine. Xenobiotica 25, 917–927.

Dahms, M., Lotz, R., Lang, W., Renner, U., Bayer, E., Spahn-Langguth, H., 1997. Elucidation of phase I and phase II metabolic pathways of rhein: species differences and their potential relevance. Drug Metab. Dispos. 25, 442–452.

Foster, B.C., Vandenhoek, S., Li, K.Y., Tang, R., Budzinski, J.W., Krantis, A., 2002. Effects of several Chinese natural health products on human cytochrome P450 metabolism. J. Pharm. Pharmaceut. Sci. 5, 185–189.

Foti, R.S., Rock, D.A., Wienkers, L.C., Wahlstrom, J.L., 2010. Selection of alternative CYP3A4 probe substrates for clinical drug interaction studies using *in vitro* data and *in vivo* simulation. Drug Metab. Disp. 38, 981–987.

Guengerich, F.P., 1999. Cytochrome P-450 3A4: regulation and role in drug metabolism. Ann. Rev. Pharmacol. Toxicol. 39, 1–17.

Huang, K.C., 1999. The Pharmacology of Chinese Herbs. CRC Press, Boca Raton, Florida, pp. 233–234.

Kashiwada, Y., Nonaka, G., Nishika, I., 1986. Tannins and related compounds. XLVIII. Rhubarb. Isolation and characterization of new dimeric and trimeric procyanidins. Chem. Pharm. Bull. 37, 2016–2021.

Koyama, J., Morita, T., Fujiyoshi, H., Korayashi, N., 2005. Simultaneous determination of anthraquinones, their 8-b -D-Glucosides, and sennosides of rhei rhizoma by capillary electrophoresis. Chem. Pharmaceut. Bull. 53, 573–575.

Law, F.C.P., Yao, M.C., Bi, H.C., Lam, S., 2017. Physiologically based pharmacokinetic modeling of tea catechin mixture in rats and humans. Pharmacol. Res. Perspect. 5, 1–18.

Lewis, D.F., Lake, B.G., 1996. Molecular modeling of cyp 1A subfamily members based on an alignement with cyp 1A2: rationalization of cyp 1A substrate specificity in terms of active site amino acid residues. Xenobiotica 26, 723–753.

Lorenzen, A., Hendel, J.D., Conn, K.L., Bittman, S., Kwabiah, A.B., Lazarovitz, G., Masse, D., McAllister, T.A., Topp, E., 2004. Survey of hormone activities in municipal biosolids and animal manures. Environ. Toxicol. 19, 216–225.

Mueller, S.O., Stopper, H., Dekant, W., 1998. Biotransformation of the anthraquinones emodin and chrysophanol by cytochrome P450 enzymes. Drug Metab. Dispos. 26, 540–546.

Pharmacopoeia of China,, 2000. Part 1. Chemical Industry Press, Beijing.

Riley, R.J., Howbrook, D., 1998. Analysis of the activity of the major human hepatic enzyme (CYP3A4) using [*N*-methyl-^{14}C]-erythromycin. J. Pharmacol. Toxicol. Methods 38, 189–193.

Safe, S.H., 1998. Hazard and risk assessment of chemical mixtures using the toxic equivalence factor approach. Environ. Health Perspect 106, 1051–1058.

Shia, C.S., Juang, S.H., Tsai, S.Y., Chang, P.H., Kuo, S.C., Hou, Y.C., Lee-Chao, P.D., 2009. Metabolism and pharmacokinetics of anthraquinones in *Rheum palmatum* in rats and *ex vivo* antioxidant activity. Planta. Med. 75, 1386–1392.

Strandell, J., Neil, A., Carlin, G., 2004. An approach to the *in vitro* evaluation of potential for cytochrome P450 enzyme inhibition from herbals and other natural remedies. Phytomed 11, 98–104.

U.S. EPA. 1999. Guidance for conducting health risk assessment of chemical mixtures, U.S. Environmental Protection Agency, Risk Assessment Forum. Washington, DC. NCEA-C-0148.

U.S. FDA Guidance for Industry Botanical Drug Products. 2004. U.S. Department of Health and Human Services, Food and Drug Administration, Center for Drug Evaluation and Research (CDER), Rockville, MD. <http://www.fda.gov/cder/guidance/index.htm>.

Venkatakrishnan, K., Moltke, L.L., Greenblatt, D.J., 2001. Human drug metabolism and the cytochromes P450: application and relevance of *in vitro* models. J Clin. Pharmacol. 41, 1149–1179.

Villeneuve, D.L., Blankenship, A.L., Giesy, J.P., 2000. Derivation and application of relative potency estimates based on in vitro bioassay results. Environ. Toxicol. Chem. 19, 2835–2843.

Yan, D.M., Ma, Y.M., Shi, R., Xu, D.S., Zhang, N., 2008. Anthraquinone pharmacokinetics in Xiexin decoction and the different combinations of its constituent herbs. Eur. J. Drug Metab. Pharmacokinet. 33, 69–75.

Yao, H.T., Chang, Y.W., Lan, S.L., Yeh, Y.K., 2008. The inhibitory effect of tannic acid on cytochrome P450 enzymes and NADPH-CYP reductase in rat and human liver microsomes. Food Chem. Toxicol. 46, 645–653.

Zou, L., Harkey, M.R., Henderson, G.L., 2002. Effects of intrinsic fluorescence and quenching on fluorescence-based screening of natural products. Phytomed 9, 263–267.